Hollow Fiber Spacesuit Water Membrane Evaporator Development and Testing for Advanced Spacesuits

Grant C. Bue[1] and Luis A. Trevino[2]
NASA Johnson Space Center, Houston, TX, 77058, USA

Gus Tsioulos[3]
Wyle Integrated Science and Engineering Group, Houston, TX 77058, USA

and

Joseph Settles[4], Aaron Colunga[5], Matthew Vogel[6], Walt Vonau[7]
Jacobs Engineering, Engineering and Science Contract Group, Houston, TX, 77058, USA

The spacesuit water membrane evaporator (SWME) is being developed to perform the thermal control function for advanced spacesuits to take advantage of recent advances in micropore membrane technology in providing a robust heat-rejection device that is potentially less sensitive to contamination than is the sublimator. Principles of a sheet membrane SWME design were demonstrated using a prototypic test article that was tested in a vacuum chamber at JSC in July 1999. The Membrana Celgard X50-215 microporous hollow fiber (HoFi) membrane was selected after recent contamination tests as the most suitable candidate among commercial alternatives for HoFi SWME prototype development. A design that grouped the fiber layers into stacks, which were separated by small spaces and packaged into a cylindrical shape, was developed into a full-scale prototype consisting 14,300 tube bundled into 30 stacks, each of which are formed into a chevron shape and separated by spacers and organized into three sectors of ten nested stacks. Vacuum chamber testing has been performed characterize heat rejection as a function of inlet water temperature and water vapor backpressure and to show contamination resistance to the constituents expected to be found in potable water produced by the distillation processes. Other tests showed the tolerance to freezing and suitability to reject heat in a Mars pressure environment.

I. Introduction

The spacesuit water membrane evaporator (SWME) is being developed to perform the thermal control function for advanced spacesuits to take advantage of recent advances in micropore membrane technology in providing a robust heat-rejection device that is potentially less sensitive to contamination than is the sublimator. In the circulating loop the SWME serves both as the coolant in the Portable Life Support System (PLSS) and the liquid cooling garment worn by the crewperson. It does this by evaporating water which would be replaced by a feedwater supply. The potential efficacy of a sheet membrane SWME design were demonstrated using a prototypic test article that was tested in a vacuum chamber [1] and have been proven in an Exploration Technology Development Project (ETDP) with a full scale prototype in a companion paper. [2] A parallel ETDP effort has been in progress to build an alternative design using a hollow fiber membrane geometry. Commercial hollow fiber technologies, both porous

[1] Aerospace Technologist, Crew and Thermal Systems Division, 2101NASA Parkway/EC2, non-member.
[2] Thermal Lead for Primary Life Support Subsystem/Space Suit and Crew Survival Systems Branch/2101 Nasa Parkway 77058/EC5/non-member
[3] Test Engineer, Bioastronautics, Wyle ISEG, 1290 hercules Drive, Suite 120, Mail Code LM14/S22
[4] Senior Technician, Crew and Thermal Systems Division, 2101NASA Parkway/EC2, non-member.
[5] Test Engineer, Test and Fabrication, 2224 Bay Area Blvd. MC JE-5EA, Non-member
[6] Thermal Analyst, Thermal and Environmental Analysis Section, 2224 Bay Area Blvd. MC JE-5EA, Non-member
[7] Thermal Analyst, Thermal and Environmental Analysis Section, 2224 Bay Area Blvd. MC JE-5EA, Non-member

and nonporous membranes, were tested for tolerance to potable water constituent concentration in the circulating coolant loop. Membrana Celgard X50-215 microporous hollow fiber (HoFi) membranes were selected after contamination tests, as the clearly superior candidate among tested alternatives for HoFi SWME prototype development. A number of design variants using the Celgard technology were considered. A design that configured the fiber layers into stacks, separated by 2 mm spaces and packaged into a cylindrical shape, was deemed by test to be best for further development. A n analysis of test data showed that eight layer stacks of the HoFi sheets that had good exposure on each side of the stack would evaporate water with high efficiency. [3,4] A design that has 14,300 tubes, with 18 cm of exposed tubes between headers has been built and tested that meets the size, weight, and performance requirements of the SWME. This full-scale prototype consists of 30 stacks, each of which are formed into a chevron shape and separated by spacers and organized into three sectors of ten nested stacks. Testing has been performed to show contamination resistance to the constituents expected to be found in potable water produced by the distillation processes. Other tests showed the sensitivity to bubbles, surfactants, and freezing. The ability of the system to reject heat in a Martian atmosphere was also demonstrated.

II. Fabrication and Assembly

The basic hollow fiber structure selected for the prototype is the Celgard X50-215 fiber sheets of the Membrana Minimodules that have been tested previously. [3] Details of the fiber structure are shown in Fig. 1. The porous polypropylene hollow fibers are stitched together in a regularly spaced parallel array about 21 per cm, see Fig. 1a. The tubes have a 300 μm outer diameter and a 40 μm wall thickness yielding a burst strength of 2760 kPa (400 PSI), see Fig. 1b. The tube walls are 40% porous consisting of typically slit-shaped openings having widths up to 0.04 μm lengths up to l10 μm. The hydrophobicity of the polypropylene and the pore geometry result in a water bubble point of greater than 276 kPa (40 PSI). Fiber arrays were obtained from the manufacturer in an 9 inch wide sheets.

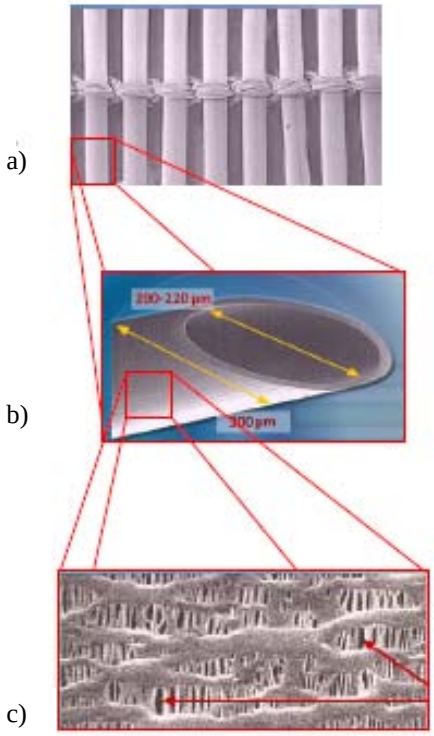

Figure 1. Magnified details of Celgard X50-215 hollow fibers. a) sheets of parallel array of tubes 52-53 per inch; b) tube cross-section, c) micrograph of pore structure

Efficiency studies showed that as the number of layers increased the evaporation on a per tube basis decreased. To minimize the volume and mass of the prototype, a optimal design element consisting of stacks of 5 layers of sheets, separated by gaps of 0.89 mm (0.35 in) was adopted. The cartridge assembly contains the chevron-shaped HoFi segments that are separated by spacer combs to allow the vapor to flow radially away from the center of the cartridge, see Fig. 2a. Within each of the three 120-degree sections of the cartridge assembly are ten chevron stacks. Major HoFi water and vapor flow passages are designed into the cartridge assembly, as shown in Fig 2b, to promote for radial outflow of the water vapor to the peripheral space between the fiber perimeter and the housing. Water vapor then flows axially parallel to the liquid water in the tubes, sed Fig 2c.

What follows is an overview of the assembly process, which is detailed elsewhere. [5] Each stack is formed by folding sheets to appropriate widths using cardboard folding guides. The guides are removed and the folded sheets are heat sealed for 4 seconds at 138 °C (280 °F) to tack each stack together at the ends and prevented potting material from plugging the tubes. The stacks are protected with a paper sleeve. With one comb placed in a cartridge groove, a set of 10 the sleeved stacks are inserted into the corresponding comb slots. A second comb is inserted at the same level with the free edges of the first set of stacks to forming 10 chevrons with 1.27 cm (0.5 in) projecting beyond the cartridge ends. The second and third sets of ten stacks are inserted into the corresponding open slots of the two combs and then formed into chevrons by inserting the third comb. Four more sets of three combs are inserted in the cartridge to define the chevrons with gaps at four more evenly spaced levels. The protective sleeves are slowly slipped off chevrons by gently pulling one end of the sleeve while holding the stack at the other end.

The cartridge is then potted successively on both ends with 70A Shore hardness polyurethane to a level 1.8 cm (0.7 in) above the cartridge rings. The fully cured potted cartridge is secured in a lathe and the ends are cut with a razor sharp blade using deionized water as a lubricant. The combs were removed from the first unit, HoFi #1 and a second unit was built with the combs left in place, HoFi #2, see Fig. 3. Inspections of the cut ends shows the tubes are all open and apparently bonded to the polyurethane, see Fig. 4. The resulting cartridge is 20.3 cm (8 in) in length with a diameter of 8.3 cm (3.25 in). The cartridge is assembled into gasket sealed inlet and outlet manifolds. The polyurethane headers have been proof tested in the manifolds to two atmospheres without leaking. An acrylic cylindrical housing separates the inlet and outlet manifolds and provides a gap for water vapor outflow at the periphery of the chevrons. The housing is clear affording view of the fibers during test and the cartridge manifold junction. The housing is fitted with a port for backpressure instrumentation. For the prototype, the cartridge cage and the manifolds were made with steel for ease of manufacturing, but would be made of acrylic for the final design.

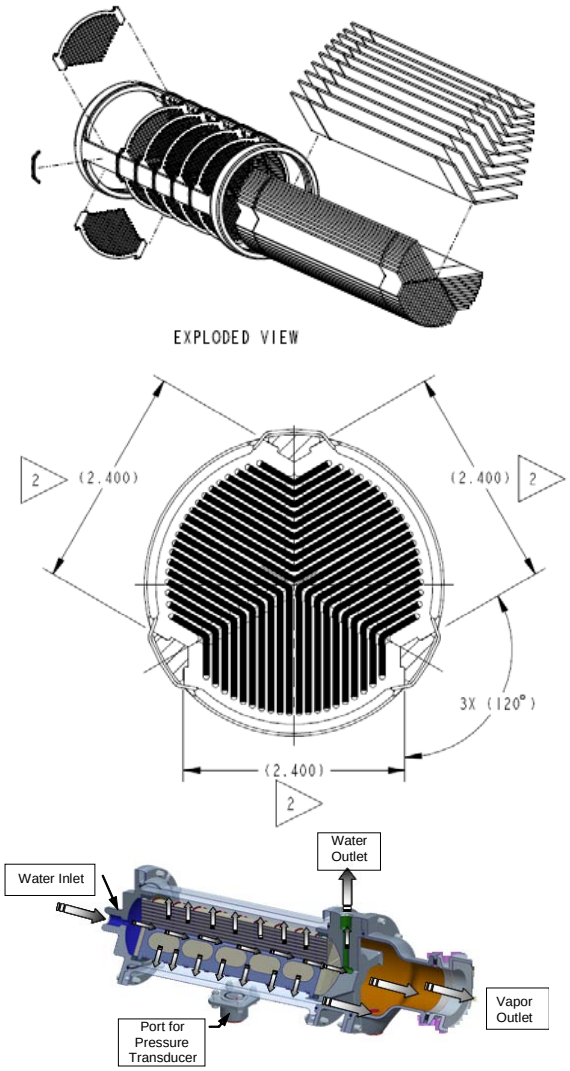

Figure 2. Selected components of HoFi SWME assembly.a) Exploded view of cartridge showing chevron stacks; b) View of 3-comb layer showing slots for 30 chevrons; c) Section of HoFi SWME showing flow paths of coolant and evaporant

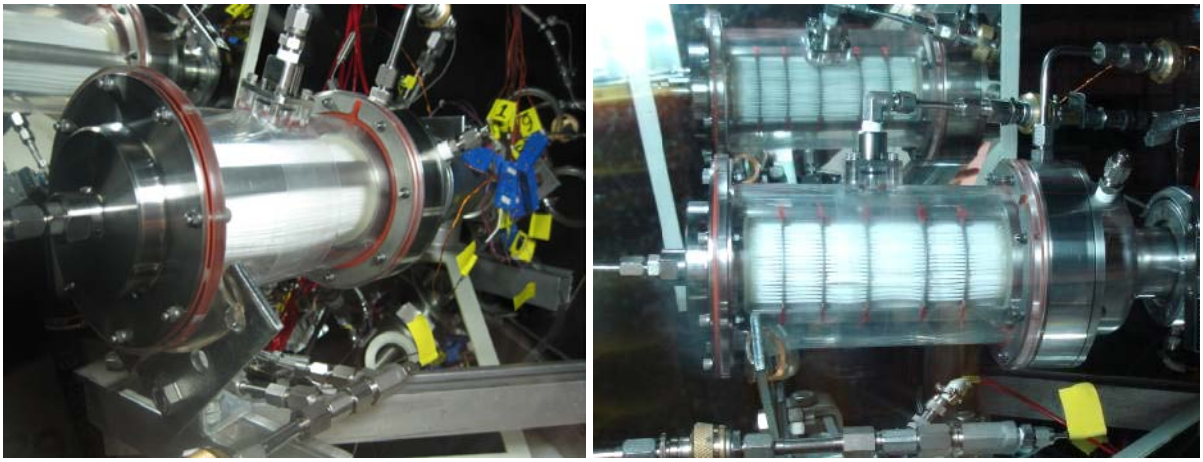

Figure 3. HoFi SWME prototypes: a) HoFi #1 (no combs); b) HoFi #2 (five comb layers)

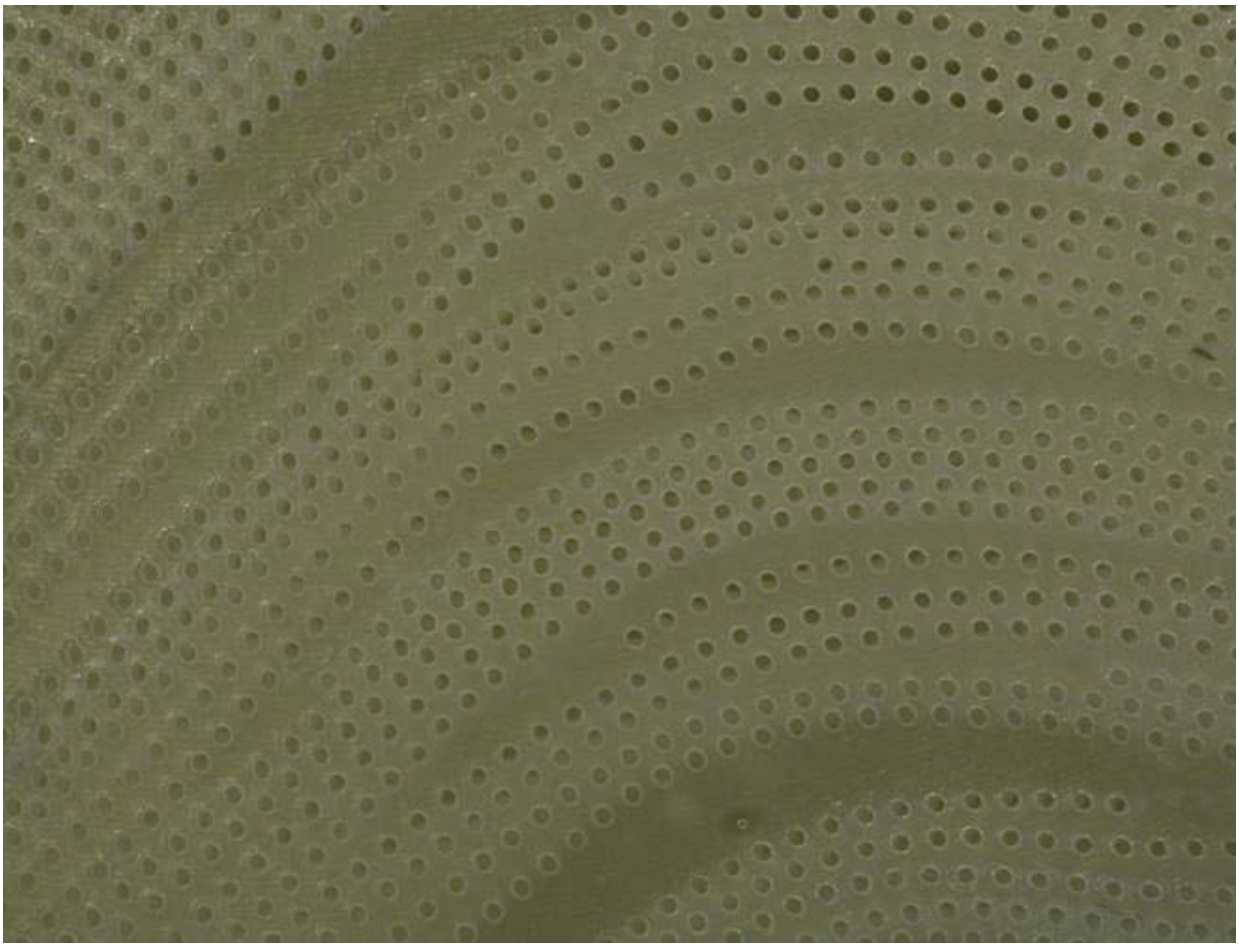

Figure 4. Magnified view of cut ends of hollow fibers in polyurethane header.

III. Test Methods

A series of four tests were conducted to assess the performance, contamination sensitivity, freeze sensitivity, and mars atmosphere performance simulations. These tests were conducted in the Building 220 vacuum chamber at the National Aeronautics and Space Administration Johnson Space Center in Houston, Texas, USA. HoFi 2 (five levels of combs) was used for the performance (except the bubble tests) and contamination testing. HoFi 1 (no combs) was used for repeat performance tests (10 psi coolant loop), bubble tests, freeze tests and mars tests.

A. Key Instrumentation

The most important measurements for the four test series were the inlet/outlet temperatures, SWME water loop mass flow, and vapor backpressure, and the instrumentation scheme was common to the different tests. Calculations of SWME heat rejections and instantaneous vapor mass flow rates were based on being able to accurately measure mass flow and temperatures. Inlet and outlet temperatures were measured with Fluke Hart Scientific 5611T thermistor probes that have an ±0.01°C accuracy. Thermistor sensors were monitored by the Fluke Hart Scientific Black Stack Model 1560 thermometer via its Fluke Hart Scientific Model 2564 thermistor scanner. These components have an accuracy of ±0.003°C. The JLC International type 1 flow meter sensor has an accuracy of ±3% of measured value and is monitored by the Precision Digital PD693 Flow Indicator. SWME backpressures were measured by a Baratron 690A 100 mmHg series, which has a worst case accuracy of 0.12% of reading.

B. Test Set-up

A similar test set-up was used for the four tests. Figure 5 is a schematic of the test loop illustrating the SWME water loop, thermal conditioning water loop, and key instrumentation. SWME water inlet temperatures were controlled by the chiller cart via a liquid to liquid heat exchanger (HX). The chiller cart also had an 800 W heater that had to be supplemented with immersion and line heaters to match the higher SWME heat rejection rates. Makeup water was continuously supplied from the reservoir feedwater tank as the SWME evaporates water.

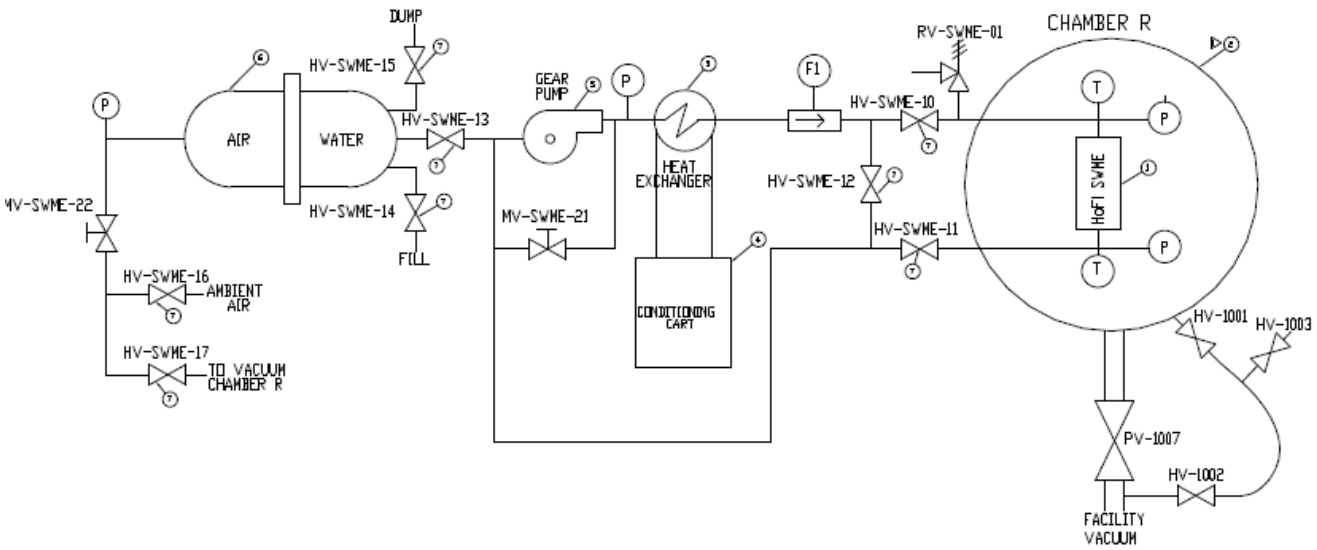

Figure 5 Test Set-up

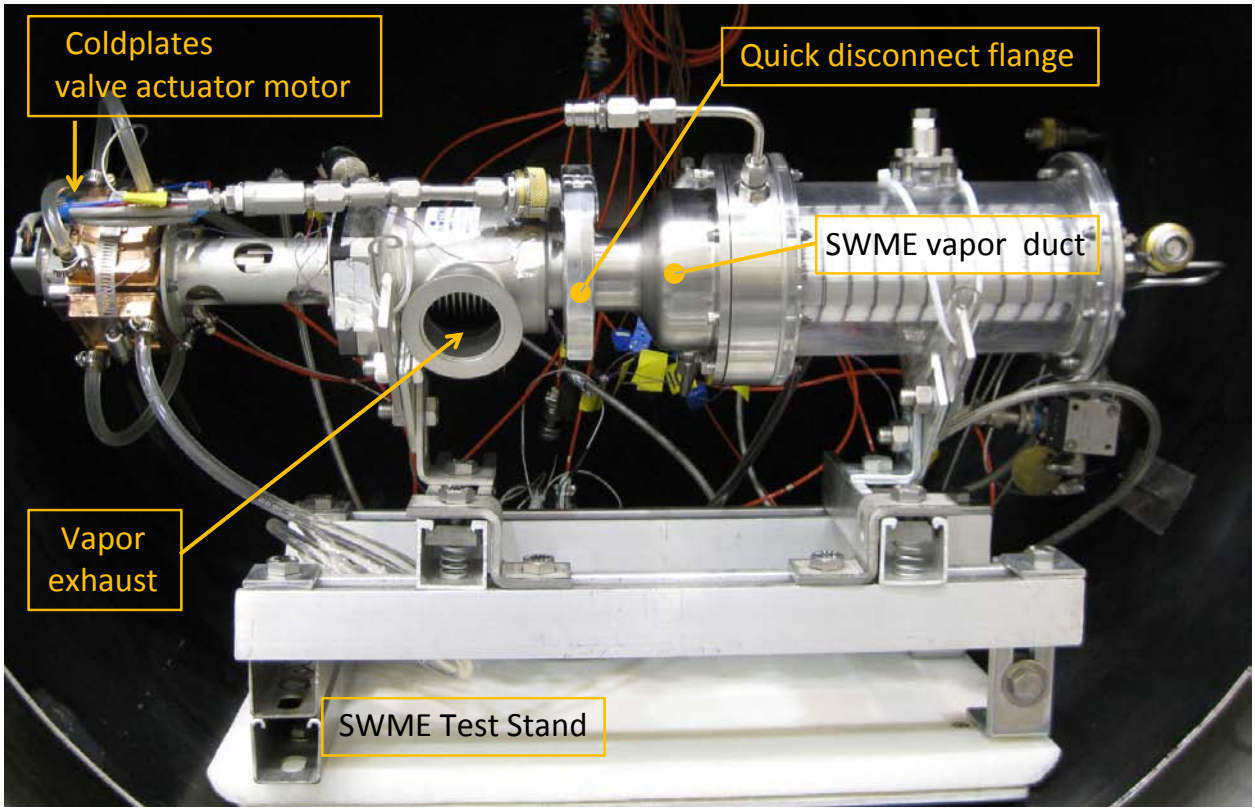

Figure 6. Backpressure control for tests

Pressure in the reservoir was adjustable allowing for variable pressures at the SWME water inlet. The reservoir was weighed daily at test beginning and end to calculate total water evaporated. Air injections were done at the sample port during bubble testing with a 50 cm^3 plastic syringe fitted with small flexible tubing. A valve controlled (not shown) at the base of the port would be opened prior to the air injection and then closed immediately afterwards. The SWME water flow was adjusted by adjusting the pump motor speed controller. SWME heat rejections rates

were controlled by the backpressure valve, which when adjusted would change the SWME vapor side pressure, also called backpressure. Backpressure valve adjustments were done via the LabView data acquisition system (DAQ).

Backpressures would range from water saturation pressure corresponding to inlet temperatures when the valve was closed to values less than the water triple point pressure when the valve was fully opened. The backpressure valve was a permanent part of the loop, see Fig. 6. Due to active use, the valve actuator motor had to be actively cooled to prevent motor overheating. Cooling water flowed through coldplates strapped to all four sides of the rectangular motor housing. Each SWME had a vapor duct with outlet flange dimensions matching the valve interface flange to allow for quick change outs.

C. Performance Tests

The HoFi SWME performance tests consisted of a set of tests characterizing the fundamental performance of the HoFi SWME. Deionized water was used for all performance tests.

The backpressure performance tests used backpressure control to examine the performance at the extremes of the expected range of coolant loop pressures, 10 psia and 21 psia, and six back-pressure settings to control the outlet temperature ranging from fully open to fully closed. Inlet temperatures were controlled to 16 °C, 20 °C, 24 °C, 28 °C, 32 °C, and 36 °C. Coolant flow rates of 91 kg/hr and 60 kg/hr were tested. A total of 72 test points were conducted to map the performance with respect to the four variables.

Bubble performance tests investigated the HoFi SWME for vulnerability to air bubbles. Air bubbles were injected into the sample port, first in the amount of 5 cm^3, then 10 cm^3, and finally 20 cm^3. After each quantity was injected into the coolant stream, the performance of the HoFi SWME was monitored until performance stabilized. Clear tubing segments allowed viewing of the inlet and outlet coolant streams for the presence of circulating bubbles.

D. Contamination Tests

The contamination test series was designed to probe for sensitivities in the HoFi SWME element to ordinary constituents that are expected to be found in the potable water source. For these tests, based on the long term performance of the Water Processing Assembly (WPA) in the International Space Station (ISS) a level was set for each impurity found that the system could comfortably meet by a factor of 2 to 5. [6] While these levels are more concentrated than those found in the potable water of the ISS, they are well below the limits set for human consumption by NASA. This worst case potable water was selected as the baseline water quality to be supplied to the feedwater tank (see Table 1). Some ordinary potable water impurities, such as the organics, are volatile while others, such as the metals and inorganic ions are more or less nonvolatile. The nonvolatile constituents are expected to concentrate in the HoFi SWME as evaporated water from the loop is replaced by the feedwater. At some point in the HoFi SWME mission lifecycle as the concentrations of the nonvolatile impurities increase, the solubility limits of one or more of the constituents may be reached. The resulting presence of precipitate in the coolant water may begin to plug pores and tube channels, ultimately affecting the HoFi SWME performance. For the purpose of project water concentrations in the circulation loop beyond baseline, it was assumed that all constituents in the evaporation process were entirely non-volatile and also that none of the constituents would plate out on metal. All constituents were to stay behind in the circulating loop. The average heat rejection rate assumed to predict the mass of water evaporated and hence the mass of constituents left behind was a conservative 470W.

To determine approximately when in the 100 EVA SWME cycle the HoFi SWME system would begin to degrade, a series of trials were conducted with progressive contamination to monitor performance and check for degradation at contamination levels predicted for 0 EVAs (baseline water quality), 33 EVAs, 66 EVAs and 100 EVAs. The first trial began with the baseline water quality for the test loop and feedwater. The HoFi SWME element will be tested for performance and degradation for 21 hours of operation. The water concentrations in the circulating loop was planned to be as in Table 1 for the four series. The make-up water within a series was always the baseline water, as it would be for successive EVAs, that is the feedwater bladder would be replenished potable water from a distillation process similar to WPA. Rather than spiking the water with 1 CFU/ml, it was assumed that the water supply would be filter through a biofilter at the supply source, and would be devoid of biocide. It was thought that handling of the water without extreme precautions would provide microbes as it had in previous testing.[3] Thus, all water was passed through a biofilter for both the circulating water and the resupply tank.

Table 1. Planned water concentrations for coolant loop.

	Units of Measure	CxP Maximum Contaminant Level (MCL)	CxP MCL Source	Baseline Water Quality (0 Hours)	33 EVAs (264 Hours)	66 EVAs (528 Hours)	100 EVAs (800 Hours)
INORGANIC CONSTITUENTS							
Ammonia	mg/L	1	SWEG	0.1	1.9216	3.7432	5.62
Barium	mg/L	10	SWEG	0.1	1.9216	3.7432	5.62
Cadmium	mg/L			0.005	0.09476	0.18452	0.277
Calcium	mg/L			1	19.216	37.432	56.2
Chlorine (Total)	mg/L			5	94.76	184.52	277
Chromium	mg/L			0.05	0.9476	1.8452	2.77
Copper	mg/L	1	SWEG	0.5	9.476	18.452	27.7
Iron	mg/L	0.3	SWEG	0.2	2.84	5.48	8.2
Lead	mg/L			0.05	0.9476	1.8452	2.77
Magnesium	mg/L			1	19.216	37.432	56.2
Manganese	mg/L	0.3	SWEG	0.05	0.9476	1.8452	2.77
Mercury	mg/L			0.002	0.03896	0.07592	0.114
Nickel	mg/L	0.3	SWEG	0.05	0.9476	1.8452	2.77
Nitrate (NO3-N)	mg/L			1	19.216	37.432	56.2
Potassium	mg/L	340	SWEG	5	94.76	184.52	277
Selenium	mg/L			0.01	0.19216	0.37432	0.562
Sulfate	mg/L	250	SWEG	5	94.76	184.52	277
Sulfide	mg/L			0.05	0.9476	1.8452	2.77
Zinc	mg/L	2	SWEG	0.5	9.476	18.452	27.7
ORGANIC CONSTITUENTS							
Total Acids	mg/L			0.5	9.476	18.452	27.7
Total Alcohols	mg/L			0.5	9.476	18.452	27.7
Total Organic Carbon	mg/L	3	SWEG	0.3	5.844	11.388	17.1
MICROBIAL BACTERIA: TOTAL COUNT							
Bacteria	CFU/mL			1	TBD	TBD	TBD
Fungi	CFU/mL			1	TBD	TBD	TBD

* EVA concentrations calculated based on 10L initial volume
** 1 EVA is equivalent to 8 hours

E. Freeze tests

Freeze testing, involved stopping water flow while keeping backpressure valve open to freeze the water contained in the water passages. Each freeze test point started with establishing steady state, low temperature SMWE performance with the backpressure valve partially open followed by pump power down and completely opening the backpressure valve. After a duration of stopped water flow, while the water pump was powered on to apply a small pump pressure head so that complete water passages blockage by ice could be ascertain. The backpressure valve was also closed at the same time, to allow the test membranes and water channels. The SWMEs were monitored during these warm up periods to determine if water leakage occurred, which would be an indication of test article damage to thaw. The duration of the zero-flow/open-valve freeze conditions was 1 minute, 3 minutes, 6 minutes, 12 minutes and 1 hour. After each test point the test article was allowed to warm up and flow re-established. Then the valve was opened wide and baseline steady state performance was established to see if the test article performance had been compromised. The freeze tests were done with HoFi 1 (no combs).

F. Cut tube test

A problem relating to system robustness is the effect of one or more of the tube leaking. Hofi #1 was tested with two fibers cut at the exit header end to determine if heat rejection performance would be affected by the damaged fibers. Two tubes at the surface of the bundle were cut, one at mid axis and one toward the outlet, producing four open cut ends. The performance was measure at the five valve positions for the 20 °C and 32 °C inlet conditions.

G. Mars atmosphere performance simulations

Testing was performed on the test article to simulate operation within a martian atmosphere. The test article was stepped through a series of test points in which the chamber pressure, outlet water temperature, backpressure valve

opening, and or dry gaseous nitrogen (GN2) sweep gas mass flow rate were varied. The HoFi 1 test article (no combs) was modified to martian atmospheric pressures were simulated by operating the chamber vacuum pumps simultaneously while bleeding air into the chamber at a controlled rate through a tee-shaped tube with the branches of the tee perforated, see Fig. 7. The perforated branches were positioned in the axial center of the test article in the void between the three chevron sectors. GN2 sweep gas was theorized as a necessary element for mars operations to prevent the buildup vapor at the elevated martian atmospheric pressures. Water flow was set to 91 kg/hr during these tests. The mars tests were also done with HoFi 1 (no combs).

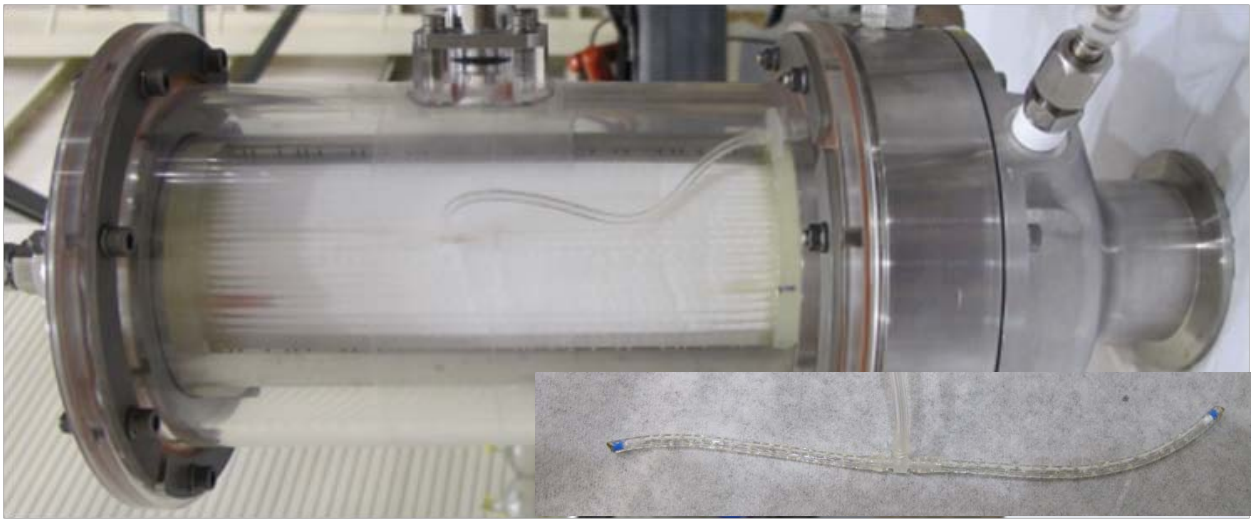

Figure 7. HoFi SWME without combs modified with sweep gas tee. Inset shows perforations in branches of tee.

IV. Results

A. Performance Tests

The extensive performance mapping test regime provided for many distinct evaluations, including varying the inlet water temperature, coolant pressure, coolant flowrate and comparisons of the HoFi #1 and HoFi#2. The heat rejection of both HoFi SWMEs with a fully open backpressure valve as a function of inlet temperature for the specification flow rate of 91 kg/hr is presented in Fig. 8. The specification heat rejection is 807 W, with an outlet temperature of 10 °C and corresponding inlet temperature of 17.7 °C is marked with a plus sign on Fig. 8. The heat rejection of the unit with combs, HoFi #2 had 3%-5% better performance than the unit without combs, HoFi#1. For HoFi #2 the heat rejection performance was linear with respect to inlet temperature. This HoFi #2 performance exceeds the specification by about 3.5%. The HoFi #1 performance is also linear except at the 32 °C inlet water temperature, which was largely due to errant valve position.

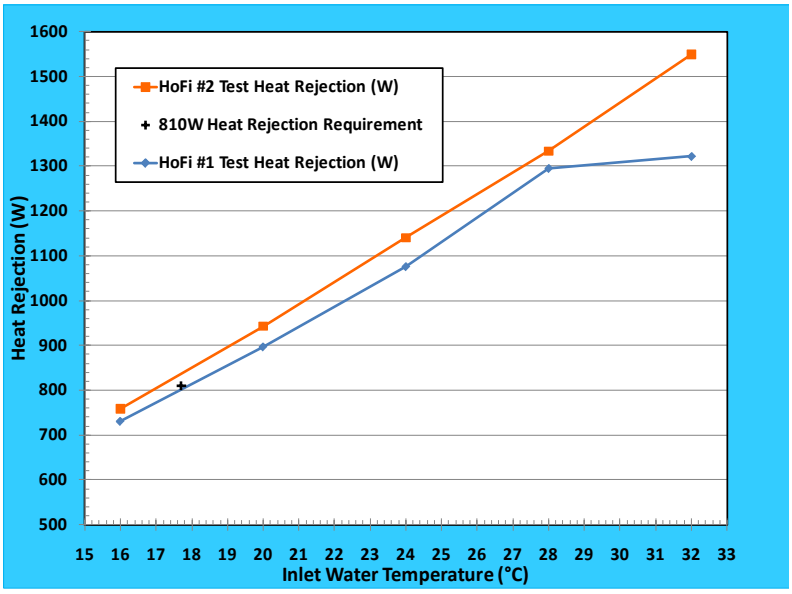

Figure 8. HoFi #2 and HoFi #1 Fully Open Valve Test Results

The heat rejection of HoFi #1 and HoFi #2 as a function of the backpressure and for a range of inlet Temperatures is presented in Figure 9. Performance over six valve

positions from fully closed to fully open were obtained for inlet water temperatures bracketing the range of inlet temperatures. HoFi #2 was able to reject 1770 W with an 36 °C inlet water which brackets conceivable conditions of the spacesuit. This is an important feature of the evaporator technology in general. As heat is stored by the human body and skin temperatures rise and coolant water temperatures rise, the ability of the unit to return the coolant loop to cooler temperatures increases. If demand suddenly increases because of heat storage and/or metabolic rate, the unit can return the coolant loop to the colder specification temperatures for peak heat rejection by the liquid cooled garment. The heat rejection of both units as a function of backpressure is nearly linear, having the about the same slope, regardless of inlet temperature. The backpressure at zero heat rejection reflects the saturation pressure at the water temperature. Some water vapor leaks occurred in early tests because of the digital valve position slipped. Figure 10 shows a comparison of the performance of the HoFi #2 at a reduced flowrate of 60 kg/hr and the specification flow rate 91 kg/hr. Both the specification and reduced flow rates produce heat rejection profiles that are nearly linear with backpressure. For a given temperature, the heat rejection negative slopes of the 91 kg/hr is always greater than that of the 60 kg/hr because for a given inlet temperature, the mean temperature and the mean driving pressure, is greater for the higher flowrate. As the water temperature increases, the differences are exacerbated. In fact 32 °C inlet temperature heat rejection at 60 kg/hr and the full open valve position is less than the 91 kg/hr heat rejection at an inlet temperature 28 °C, 4 °C less. The difference in the peak heat rejection at these two flow rates ranged between 18%, for an inlet temperature of 32 °C, to 14% at an inlet temperature of 20 °C.

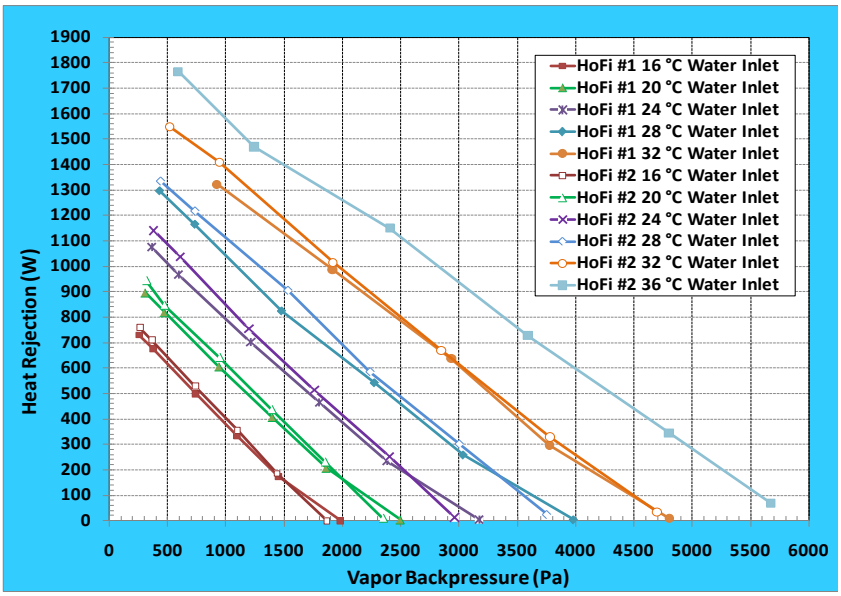

Figure 9. HoFi #1 vs. HoFi #2 SWME Heat Rejection (W) 91 kg/hr Water Mass Flow, 10 psia Water Pressure

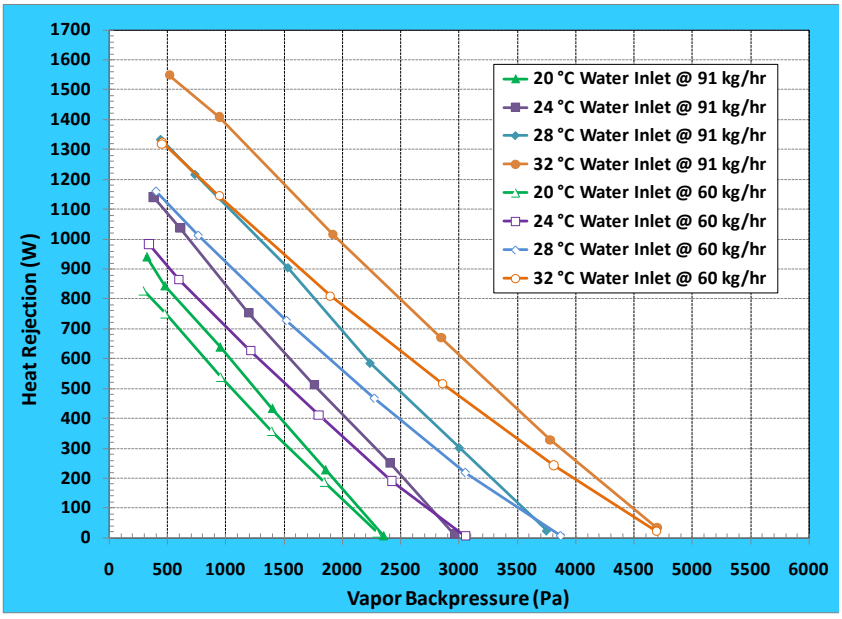

Figure 10. HoFi #2 heat rejection as a function of vapor backpressure and flow rates of 91 kg/hr and 60 kg/hr.

The average difference in heat rejection across the range of backpressures at the extremes of coolant pressure, 21 psia and 10 psia, is less than 0.5% at the specification flowrate (data not shown). This suggests that the fibers do not deform significantly at the higher pressure.

Bubble tests were conducted with HoFi #1 in which varying amounts of air were injected into the supply water line well upstream of the test article. The water supply and return lines

each had a section of clear tubing near the test article so that bubbles could be visualized going into the test article and also whether or not bubbles exited. HoFi #1 was subjected to up to 50 cc of air injections into the 91 kg/hr water flow while maintaining the backpressure valve at three valve positions (fully closed, partially open, fully opened) for two different water inlet temperatures (20°C, 32°C). For all test points, no bubbles were seen exiting the test article. Each SWME effectively expelled all gas into the vacuum chamber via its porous membranes. All air injections were completed within five seconds or less.

Unfortunately, the sample rate of these tests were too slow to catch the transients effectively, but in one of the test series the transients were partially captured. Figure 11 captures some of the transient responses of the 10 cm^3 and 50 cm^3 bubble injections from the 20 °C fully open test series. These transients occurred within a 40 second period following the injection. The flow rate and the heat rejection dip in synchrony presumably because of the displacement of the coolant with the air injection. This is also possibly due to partial blocking of the pores with air—note the decline in the vapor backpressure that starts and the beginning of the 5 cm^3 and ends following the transient response to the 50 cm^3 injection, see the right angle arrows in Fig 11. In the case of the fully closed valve positions, the large injections resulted in backpressure that was retained until the valve was reopened (data not shown).

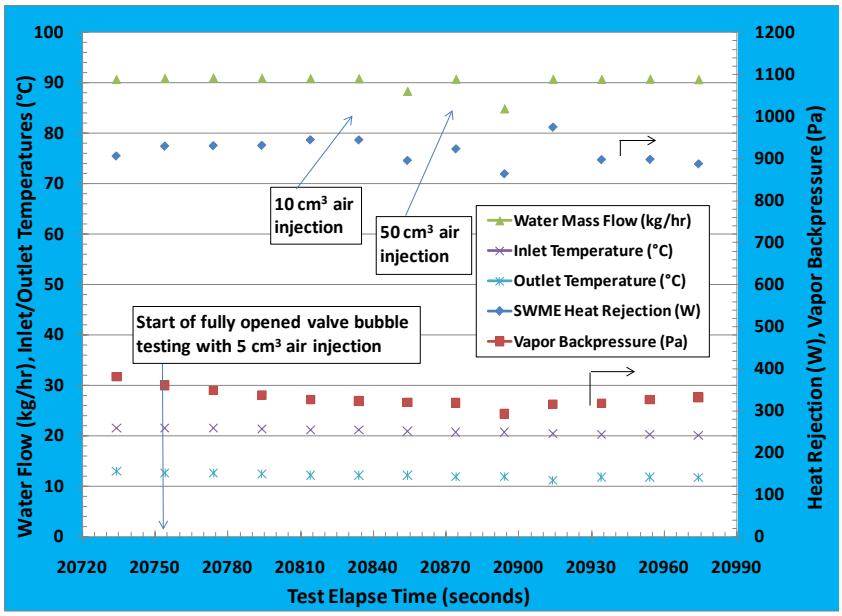

Figure 11. HoFi #1 bubble test with fully open backpressure valve and 20 °C water inlet.

B. Contamination Tests

Taking the HoFi #2 to the full open valve position at the beginning and end of each test day was started on Day 3 of the Baseline test, the last day of baseline testing, so comparisons at that valve position start on that day. There were three major anomalies of the contamination test. The first anomaly was that the concentration of the total acids and organics was 1000 time the intended concentration. This cause some of the copper fittings to corrode and turned the water bluish green which in turn stained portions of the membrane. The performance of the units was apparently unharmed, although it could be argued that it had increase slightly from previous performance tests using deionized water. This errant baseline water was flushed out thoroughly before proceeding with 33 EVA water tests. The second anomaly occurred at the 66 EVA water test series which was erroneously a mixture of 66 EVA water and 33 EVA water. The third anomaly occurred on day 2 of the 100 EVA water test, a pressure spike was seen at the very beginning of the day. The water loop pressure spiked to over 100 kPa while the heat rejection dropped to roughly 65% of the expected total. The test was stopped and the unit was taken out and inspected. There was a great deal of particulate matter in the inlet header area and it is believed that an event occurred that dislodged a mass from somewhere upstream in the loop, which then broke up against the inlet to the HoFi tubes inside the header. This water was cultured for the presence of microbes but there was no detectable colony forming units. The unit was briefly connected in reverse so that the water loop might be used to flush out the inlet header and tubes. Then the unit was returned to its nominal configuration and testing resumed.

The contamination heat rejection performance is charted in Figure 12 with a heat rejection axis range of 900 W to 960 W to highlight small but apparent degradation. The baseline performance was even greater than it had been in performance tests (955 W compared to 942 W). The largest apparent degradation occurred after the initial change from baseline water to 33EVA water. However, once the switch was made to 33 EVA water, the units continued to perform at roughly the same level through the 66 EVA water series. The 100 EVA water showed a slight decay both from the previous series and an average degradation from Day1 to Day3 of 0.54%. While apparently small, if

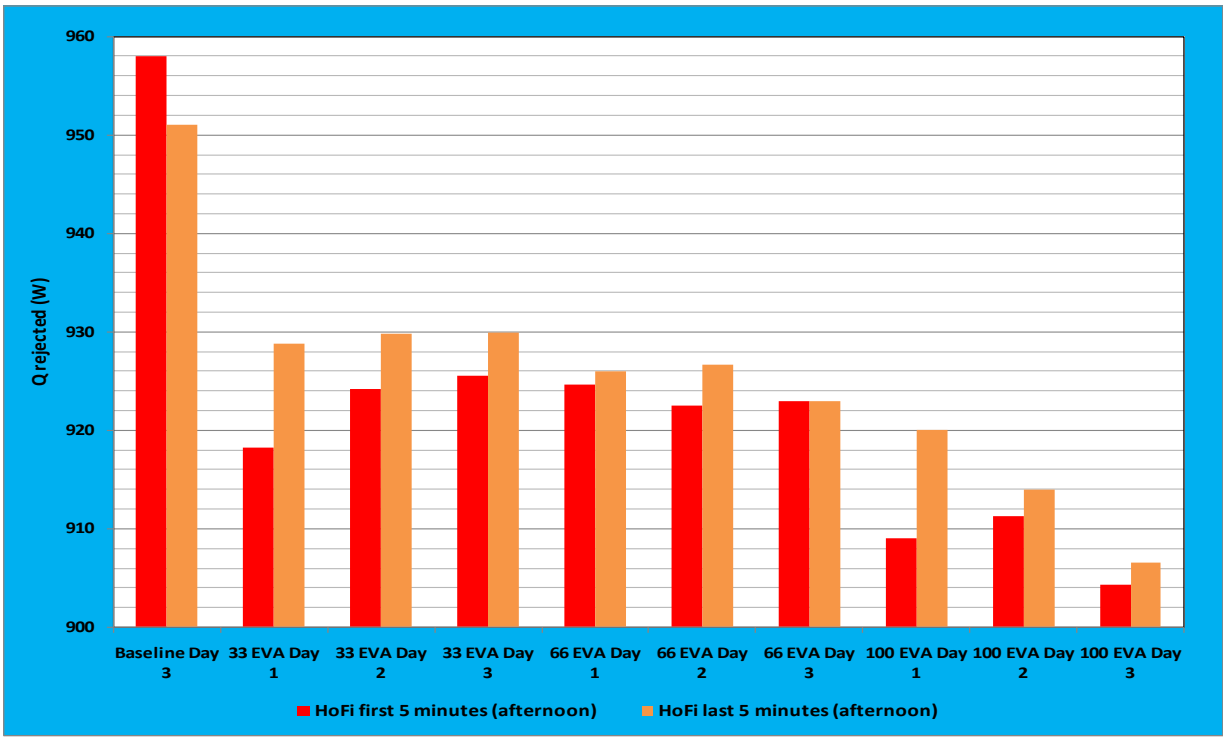

Figure 12. HoFi #2 contamination test heat rejection with fully open backpressure valve.

true this would imply that the unit should be built with a 15% margin to overcome degradation between EVA 66 and EVA 100. Another option would be to drain and flush the coolant loop 50 EVAs. Because the plugging event of the third anomaly makes it difficult to discern if this degradation is truly the result of contamination build-up at the pores or tube plugging at the inlet manifold, it is recommended that a 10-day series should be performed starting with 90 EVA water to see if performance measurably degrades in the later part of the 100 EVA life cycle.

A delta P gauge was installed in the test loop after the baseline testing was completed, so records of delta P across the liquid side was logged beginning with the 33 EVA test points. With the notable exception of the partial plugging event, the delta P of the unit was 18068 Pa ± 294 Pa. While delta P did not increase through the contamination test points, it significantly exceeds the requirement of 13742 Pa. This large pressure drop is surprising since the hydrodynamic design of the unit suggests a pressure drop of 7959 Pa, well under the requirement and close to a desired pressure drop of less than 6870 Pa. However an analysis of the manufacture pressure drop for commercial units shows the these too are 2.3 times the value predicted by hydrodynamics. Perhaps something related to the flow through small diameter porous hydrophobic tubes is responsible for the non-classical pressure drop. At least the methods used to fabricate the HoFi #1 and HoFi #2 did not introduce constrictions that were not

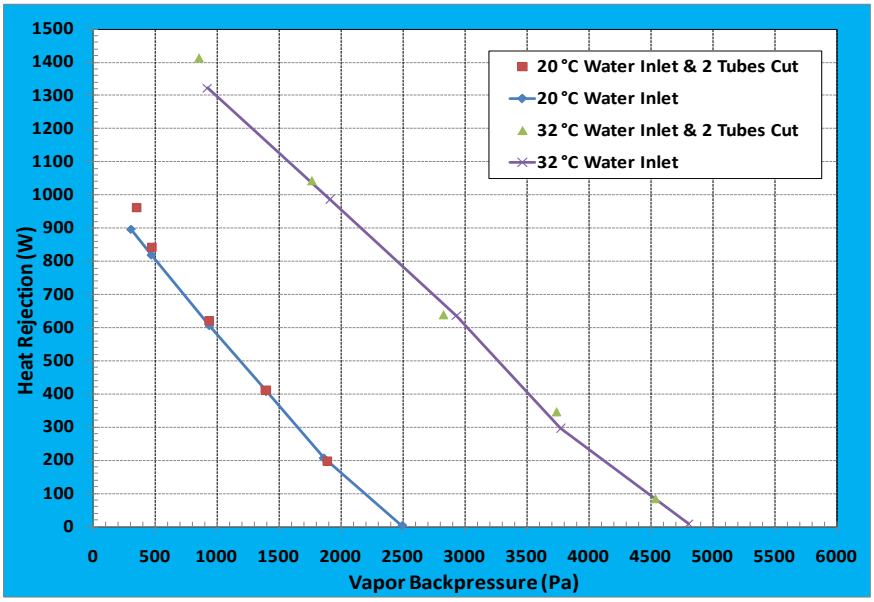

Figure 13. Heat rejection of HoFi #1 intact and with two tubes cut

present in commercial units.

C. Cut tube test

Prior to depressing the chamber, water droplets were observed at the end of the cut fibers with the flow at 45 kg/hr. After chamber depress, water was observed squirting out of the fiber ends when the flow was increased to 91 kg/hr. Differences between the baseline performance mapping and cut fiber test heat rejections are minimal except at the fully open valve test points, see Fig. 13. This could be due to the additional sublimation occurring from ice accumulated on the fibers surrounding the cut ends. The normal performance mapping reflects the fact that the uncut tubes were uncompromised by the two cut fibers. This is further supported by the freeze test which were subsequently performed with the same test article, modified by sealing the cut ends with epoxy. The recovery from freeze showed performance that mapped closely to the baseline, and there was no leaking in this test from tubes near the sealed ends. There was, however, a substantial reduction in water utilization as might be expected. The normal utilization, which typically was about 93%, dropped to 73% in the cut fiber test. This amounts to about 640 ml of water outflow from just 2 cut fibers when the intact flow rate was less than a tenth. Two cut fibers produce four ends exposed to about a 10 psi delta pressure. The combination of the higher delta pressure and four open ends results in this significant leakage.

D. Freeze Tests

HoFi #1 was allowed to freeze, by opening the backpressure valve fully and stopping flow. Freezing of the membranes as measured by externally mounted thermocouples, occurred within a minute. The freezing condition was allowed to occur in four successively longer tests, for 1 min, 3 min, 6 min, 12 min and 1hour, each test followed by the closing the backpressure valve until the unit warmed up and flow could be re-established. Full open heat rejection was then monitored to see if performance had degraded.

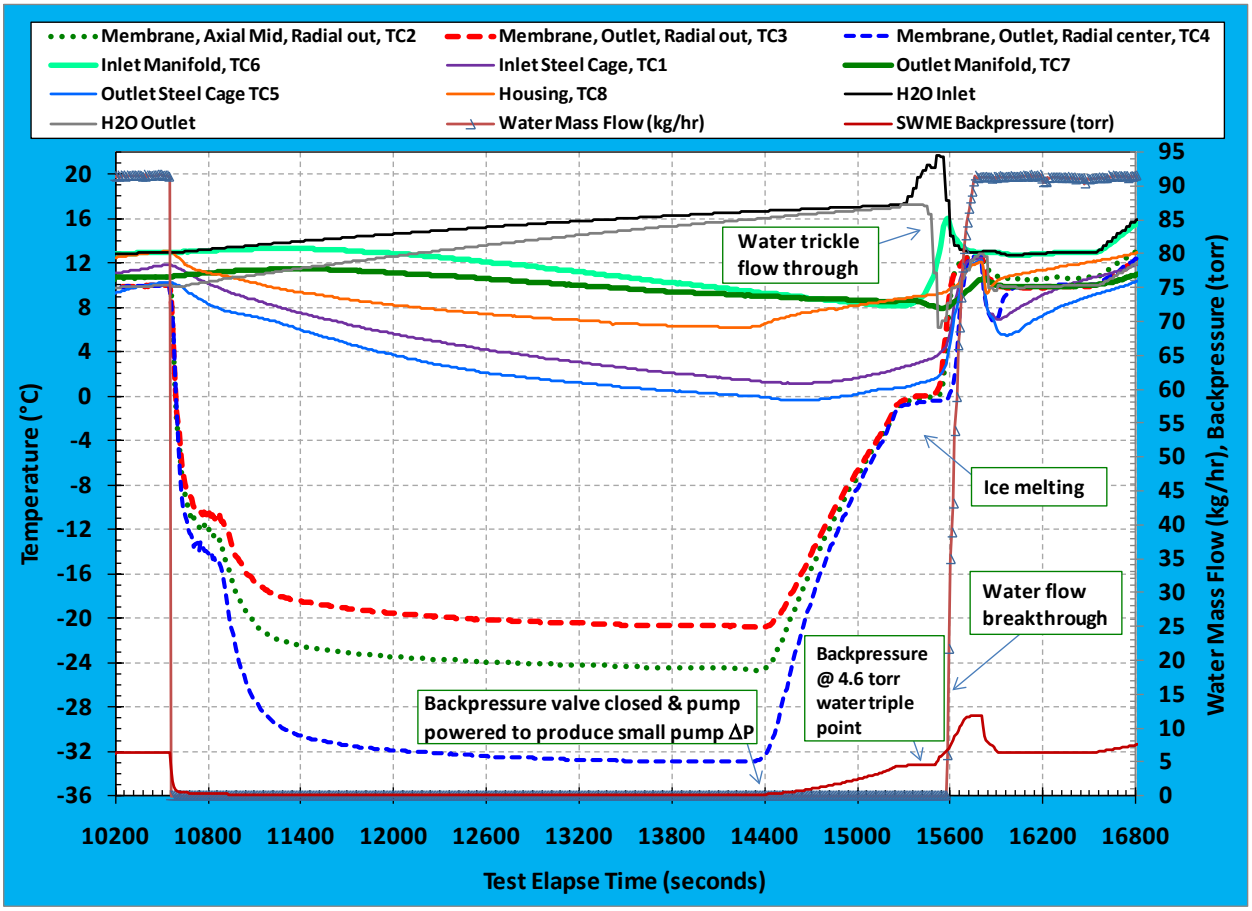

Figure 14. HoFi #1 one hour freeze test results

HoFi #1 one hour freeze test results are plotted in Figure 14. Membrane temperatures dropped quickly past 0°C, and then experienced a plateau or decreased cool down rate a little more than two minutes after pump shutdown. Why this pause would happen let alone occur at membrane temperatures around -12°C remains unknown. The radially centered membrane reached the coldest temperature of -33°C while the outer circumferential membrane measurements reached minimum of -21°C and -25°C. Radially outward membrane warmer temperatures result from their view the housing, which remained up to 31°C warmer. Given its proximity to the outlet header, the radially outward membrane near the outlet header was influenced by the warmer header and, not surprisingly, 4°C warmer than its counterpart located at the axial middle. The HoFi cage (internal) structure near the outlet and inlet headers have a relatively strong conduction heat transfer path to the headers and reached 0°C and 2°C, respectively. These temperatures demonstrate the potential of freezing occurring in the headers which in the room temperature chamber conditions would begin about 3 hours after freeze conditions began. About 10 minutes after the backpressure valve had been closed, 91 kg/hr flow was re-established to the unit. At this point a small leak (about 1 ml) was observed at the outlet header which stopped a few minutes later upon header and water temperature rises. No further leaks were observed during testing performed the following day, the final day of HoFi #1 testing..

The freeze test results demonstrated significant membrane robustness. The HoFi membrane, sheet or hollow fiber, might be resistant to catastrophic failure because the freezing water could expand through the pores and is not contained within a bounded volume. It is also possible that the plastic membranes are experiencing plastic deformation when subjected to water freezing cycles.

E. Martian Atmosphere Simulation

Testing was performed to simulate operation within a Martian atmosphere. HoFi #1 was stepped through a series of test points in which the chamber pressure, outlet water temperature, backpressure valve opening, and or dry gaseous nitrogen (GN2) sweep gas mass flow rate were varied. Martian atmospheric pressures were simulated by operating the chamber vacuum pumps simultaneously while bleeding air into the chamber at a controlled rate. GN2 sweep gas, as a test surrogate for carbon dioxide, was theorized as a necessary element for Mars operations to prevent the buildup vapor at the elevated Martian atmospheric pressures. Water flow was set to 91 kg/hr during these tests. At low elevations, Martian atmosphere ranges annually from 670 Pa to about 1000 Pa. This test used pressures close to the annual mean, 800 Pa, and 1300 Pa, a pressure well above the Martian extreme.

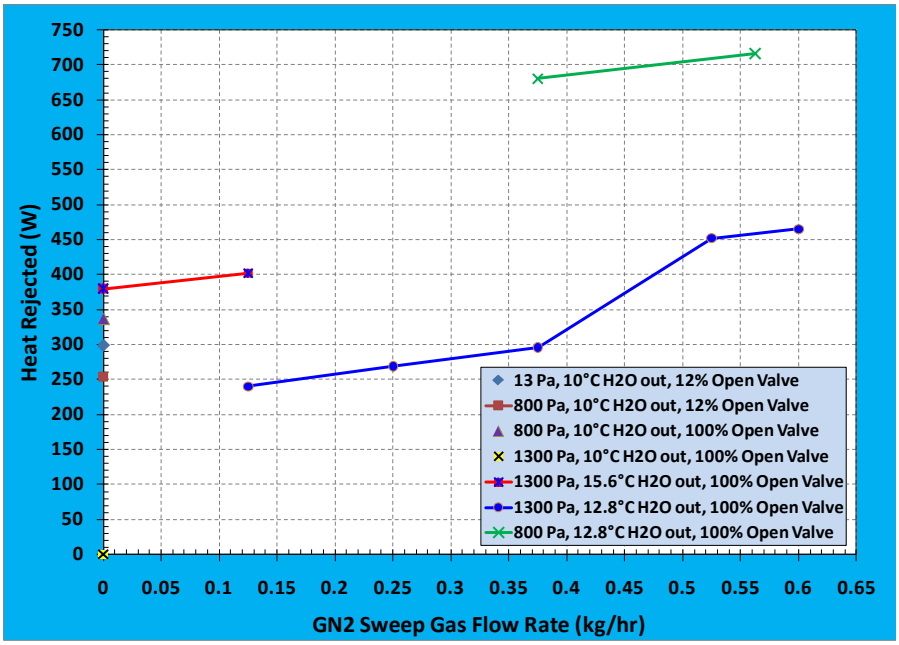

Figure 15. HoFi #1 Martian atmosphere heat reject with and without nitrogen sweep gas

The result of this test is plotted in Figure 15. Five test points were conducted with no sweep gas flow. At 1300 Pa and an outlet temperature of 10 °C, the heat rejection was zero, because the water vapor saturation pressure was 1227 Pa, less than the external pressure. The only evaporation in this case was due to diffusion and thus effectively no heat rejection occurred. With valve 12 % open, at 800 Pa external pressure, with the water at 10 °C the HoFi #1 rejected 254 W, 85% of the heat rejection at near vacuum chamber pressure for that valve position. Opening the valve completely, the unit was able reject 337 W. The mean saturation pressure was about 1370 Pa and the external pressure of 800 Pa, resulted in a positive pressure gradient between the HoFi #1 and the chamber of 570 Pa, which was sufficient to self-sweep the unit to some extent. Similarly with an inlet of 15.6 °C, and an external pressure of 1300 Pa, the effective gradient due to the mean saturation pressure was about 700 Pa resulting in 380 W.

It was reasoned that in the cold partial pressure environment of Mars, that more heat leak could be designed into the suit during high metabolic rate cases. If this were true then a higher outlet temperature could be used, because the heat requirement through evaporation would be less, and therefore performance at outlet temperatures of 12.8 °C were investigated. The solid blue line of Figure 15 shows the effect of sweep gas at 1300 Pa external pressure on heat rejection, with a 12.8 °C outlet temperature. The shift in apparent performance that occurred in changing GN2 flow from 0.375 to 0.525 kg/hr was due to the better control that was obtained over the sweep gas flow resulting in with improved measurement accuracy. It is clear from the 800 Pa external pressure case, see the green line in Fig. 15, that sweep gas had a secondary effect: extrapolating back to 0 flow the HoFi 1 would have rejected about 610 W. The sweep gas at 0.56 kg/hr only increased the rejection by about 17%. With this higher outlet temperature, most heat rejection needs could be accomplished without a sweep gas, and the sweep gas could be employed intermittently to reject extreme heat loads.

V. Conclusion

Performance characterization showed that the HoFi #2 SWME met the heat rejection requirement with a 3.5% margin. As backpressure decreased in response to the valve opening to the fully open position, the heat rejection increased linearly for a given temperature, suggesting that backpressure control would be useful for controlling outlet temperature to achieve heat rejection over the entire range of desire heat rejection rates. As inlet temperatures increased a parallel linear response was obtained, but with higher heat rejection rates for equivalent valve positions. The performance with combs was only 4% better than without combs at the specification inlet temperature, indicating that while gaps help performance, tube spatial density is more important in heat rejection. The HoFi technology is freeze tolerant, clears gas from the coolant loop without interrupting performance, and fails in a robust way should a leak occur from one or more of the tubes. The fabrication methods are flexible with respect to geometry, and can be adapted for other applications. The Mars atmosphere simulations were especially promising, achieving 716 W at 0.56 kg/hr sweep gas flow test point, only 12% less than the 810 W requirement, and only 25% less with no sweep gas at average low elevation Mars external pressures. Another positive feature is the rising HoFi heat rejections in response to increasing sweep gas flow rates. This is especially encouraging given the HoFi sweep gas implementation was done quickly due to cost and schedule constraints and is considered well less than optimized.

Contamination tests showed little degradation throughout the entire series. In the final series, an apparent degradation 0.54% per day occurred between the first and third days of the 100 EVA series. Further testing is recommended to determine if the degradation is real, and if so either a margin of 15% should be built into the flight design, or a plan to flush the coolant loop water with baseline water after 400 hours of operation. Plugging that occurred in the final series was probably the result of the sloughing off of a biofilm which had died from elevated nickel and zinc contaminants in the final series water. Filters in the coolant loop would mitigate this problem, although the test design probably exacerbated the biofilm growth. In ordinary operation the volatile organic constituents added would quickly evaporate from the system, but in the contamination test each of the four progressive series assumed all organic constituents were non-volatile.

The coolant pressure drop across the units, although consistent, was 2.3 times higher than predicted by analysis and exceeded the requirement by 31%. This can be corrected by reducing the design length by 5 cm and adding 9000 tubes, producing a pressure drop of 7650 Pa and also meeting the other system requirements.

References

[1]Ungar, E. K., and Thomas, G. A., "Design and Testing of a Spacesuit Water Membrane Evaporator," *Proceedings of the 2001 Nation Heat Transfer Conference*, ASME, Jun 2001, Anaheim, Calif.

[2]Vonau Jr., W. L., Vogel, M. R., Conger, B. C., Dillon, P. A., Zapata III, A. F., Trevino, L. A., Bue, G. C., "Sheet Membrane Spacesuit Water Membrane Evaporator Design and Thermal Tests," *Proceedings of AIAA 40th International Conference of Environmental Systems*, AIAA (to be published).

[3]Bue, G. C., Trevino, L. A, Tsioulos, G., and Hanford, A., "Testing of Commercial Hollow Fiber Membranes for Spacesuit Water Membrane Evaporator", *International Conference on Environmental Systems (ICES)*, Society of Automotive Engineering (SAE) International, Savannah, Georgia, 2009.

[4]Bue, G. C., Trevino, L. A., Hanford, A. J., and Mitchell, K., "Hollow Fiber Space Suit Water Membrane Evaporator Development for Lunar Missions", 2009-01-2371, *International Conference on Environmental Systems (ICES)*, Society of Automotive Engineering (SAE) International, Savannah, Georgia, 2009

[5]Vonau Jr., W. L., Vogel, M. R., "Testing of Commercial Hollow Fiber Membranes for Spacesuit Water Membrane Evaporators Test Report," Engineering Sciences Contract Group Memorandum, ESCG-4470-10-TEAN-DOC-0016, February 26, 2010.
[6]Carter, L., Tabb, D., and Perry, J., "Performance Assessment of the Exploration Water Recovery System," *Proceedings of the 38th International Conference on Environmental Systems*, 2008-01-2140, Jul 2008.